

## Submicron Plasticity: Yield Stress, Dislocation Avalanches, and Velocity Distribution

Péter Dusán Ispánovity,<sup>1,2,\*</sup> István Groma,<sup>1</sup> Géza Györgyi,<sup>1</sup> Ferenc F. Csikor,<sup>1</sup> and Daniel Weygand<sup>3</sup>

<sup>1</sup>*Department of Materials Physics, Eötvös University Budapest, H-1517 Budapest POB 32, Hungary*

<sup>2</sup>*Paul Scherrer Institut, CH-5232 Villigen PSI, Switzerland*

<sup>3</sup>*Karlsruhe Institute of Technology, IZBS, Kaiserstraße 12, D-76131 Karlsruhe, Germany*

(Received 13 April 2010; published 19 August 2010)

The existence of a well-defined yield stress, where a macroscopic crystal begins to plastically flow, has been a basic observation in materials science. In contrast with macroscopic samples, in microcrystals the strain accumulates in random bursts, which makes controlled plastic formation difficult. Here we study by 2D and 3D simulations the plastic deformation of submicron objects under increasing stress. We show that, while the stress-strain relation of individual samples exhibits jumps, its average and mean deviation still specify a well-defined critical stress. The statistical background of this phenomenon is analyzed through the velocity distribution of dislocations, revealing a universal cubic decay and the appearance of a shoulder due to dislocation avalanches.

DOI: [10.1103/PhysRevLett.105.085503](https://doi.org/10.1103/PhysRevLett.105.085503)

PACS numbers: 62.25.-g, 45.70.Ht, 61.72.Lk, 64.70.qj

Understanding the nature of irreversible plastic deformation is a crucially important issue in current research in materials sciences. It has been known for a long time that macroscopic size materials begin to yield at a certain stress level, depending on several material parameters. On macroscopic scales the flowing regime is traditionally described by constitutive laws, envisaging plasticity as a smooth and steady flow in both time and space. In the past decade, however, a completely new picture has emerged. By analyzing the emitted sound waves during deformation, it was observed that plastic deformation is characterized by intermittent bursts of activity [1,2]. Furthermore, recent compression tests carried out on Ni microcrystals [3,4] revealed that, if the specimen size is in the range of several  $\mu\text{m}$  and below, discontinuous deformation occurs in strain bursts due to the sudden motion of dislocations. The size distribution of the dislocation avalanches decreases by a universal power law with exponent 1.5. The distribution was recovered by experiments [5,6], by 2D and 3D discrete dislocation dynamics simulations [1,7,8], and by analytical modeling [9,10]. These findings indicate that intermittent dislocation avalanches are an intrinsic feature of the plasticity of crystals not affected by the details of the deformation.

In nanoscale applications this behavior has two important consequences. First, the increased relative size of the fluctuations makes it difficult to control the plastic forming process [7]. Second, at small specimen sizes the yield stress is not well defined any more. According to the conventional definition, the yield stress of a specimen is the external stress at 0.2% plastic strain. If the specimen size is below several  $\mu\text{m}$ , then, as a result of strain fluctuations, this value varies specimen by specimen [5] prohibiting a material-specific yield stress definition. One can thus raise the question of whether a new physical definition can be given for the yield stress at this size.

Similar phenomena are observed in completely different physical systems, too. Granular materials, such as sand piles, also exhibit yield stress, and at higher external driving forces deformation occurs in distinct avalanches [11]. Plate tectonics [12], fracture dynamics [13], and vortex lattices in superconducting films [14] are further examples of such processes. The common characteristics of these systems are marginal stability, power-law distributions without characteristic length or time scales, and driving forces that vary much slower than the internal relaxation processes [15]. For such problems the term “self-organized criticality” is widely used [16,17].

Although irregular plastic response of submicron crystalline materials is by now conceived as a self-organized critical phenomenon [4,7,15,18], a physical understanding, that is, a phenomenology for plastic flow based on statistical properties of strain avalanches, is still lacking. In this Letter we present a statistical analysis of the fluctuating stress-strain response of individual specimens and of the velocity distribution  $P(v)$  of dislocations. Our main proposition is that the  $P(v)$  holds the key to many empirical aspects of the flow. It exhibits a specific transition at the onset of material yielding seen on the average stress-strain characteristics.

The dynamics of dislocations is commonly assumed overdamped [19]. That is, the glide velocity is proportional to the glide component of the acting Peach-Koehler force  $F_g$  per unit length:  $v = B^{-1}F_g$ , where  $B$  is the drag coefficient of the dislocations. Here  $F_g = b\tau_{rs} + F_s$ , where  $b$  is the magnitude of the Burgers vector and  $\tau_{rs}$  is the sum of the external and local resolved shear stress, generated by the other dislocation segments via long-range interactions, while  $F_s$  denotes the short-range forces related to dislocation self-interaction and junction formation [19].

To study the submicron plastic response by discrete dislocation dynamics we simulated in 3D several realiza-

tions of the yielding of an  $L = 0.46 \mu\text{m}$  edge size aluminum cube oriented for single slip and compressed with constant stress rate and free side boundaries [19]. The initial dislocation density was  $8 \times 10^{13} \text{m}^{-2}$ . Part of a typical configuration is shown in Fig. 1(a) (for a movie, see [20]). Motivated by the fact that in 2D the avalanche size distribution was found to be similar to the 3D case [1,10], simulations on 2D systems consisting of straight parallel edge dislocations, oriented for single slip with periodic boundary conditions, were also performed. A typical 2D system is seen in Fig. 1(b) [20]. Although several 3D ingredients, such as dislocation multiplication, junctions, and forest dislocations, are absent from the 2D system, there is reason to expect that the essential features governing strain avalanches are included in the 2D case. Therefore, besides the much lower computational cost, an important advantage of the 2D simulations is that the role of long-range interactions in irregular plastic yielding is isolated, so its effects can be better studied.

The plastic strain responses measured during individual stress-controlled 3D simulations are seen in Fig. 2(a) (thin lines). The obtained stress ( $\tau_{\text{ext}}$ ) versus plastic strain ( $\gamma$ ) curves exhibit random steps, just like the ones measured experimentally by microcrystal deformation [3,4]. The plateaus clearly indicate strain bursts, resulting in different patterns for different samples excluding any practical definition of a threshold value. If, however, we average over the more than 100 independent realizations of submicron samples, the cavalcade of random staircases smoothens into a continuous curve, the thick line of Fig. 2(a). Moreover, there is a threshold stress value  $\tau_c \approx 65 \pm 10 \text{MPa}$  marking the end of the pure power region [inset of Fig. 2(a)]. The onset of the flow is even more evident in the deformation rate  $\dot{\gamma}$  versus external stress relation, plotted in Fig. 2(b), undergoing a quite sharp transition at the same  $\tau_c$ . Furthermore, the root mean square fluctuations of plastic strain values at given stresses [Fig. 2(c)] sharply increase for  $\tau_{\text{ext}} > \tau_c$ .

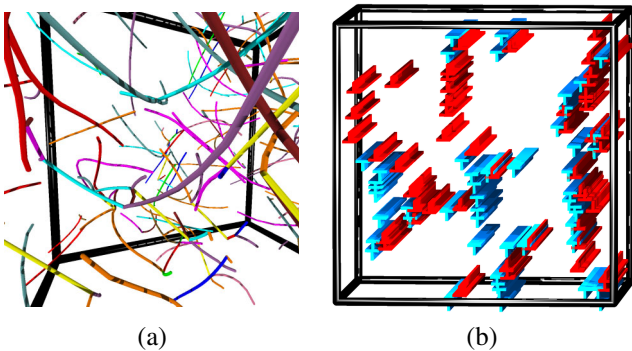


FIG. 1 (color online). Dislocation configurations obtained by 2D and 3D simulations. (a) Snapshot of a 3D simulation. Different shades (colors) indicate dislocations on the 12 different slip systems. (b) Snapshot of a 2D system consisting of straight parallel edge dislocations with Burgers vector  $(\pm b, 0, 0)$ , the sign distinguished by different shapes (colors).

Remarkably, in 2D we obtain very similar results. For each of the 5000 realizations, 64-64 opposite dislocations of a single glide axis were randomly placed initially. After letting the system relax at zero external stress, stress-controlled loading was applied. In contrast to 3D, in 2D all the material parameters can be scaled out by introducing natural units as  $v_0 = \sqrt{\rho} B^{-1} G b^2$  for velocity,  $\gamma_0 = b\sqrt{\rho}$  for plastic strain and  $\tau_0 = G b\sqrt{\rho}$  for stress, where  $\rho$  is the total dislocation density and  $G$  is a combination of elastic moduli [21]. As in 3D, the individual curves are steplike [Fig. 3(a)], but again a relatively sharp transition point can be identified on the external stress dependence of the average plastic strain [inset of Fig. 3(a)], on the deformation rate  $\dot{\gamma}$  [Fig. 3(b)], and also on the plastic strain fluctuation [Fig. 3(c)]. For 128 dislocations the critical stress obtained is  $\tau_c \approx (0.17 \pm 0.02)\tau_0$ . The outstanding similarity between the strain responses of 2D and 3D systems observed in Figs. 2 and 3 suggests that the simplified 2D case, containing only the long-range interactions between dislocations, is able to capture the general features of submicron plastic flow. We can conclude that not only is there in the statistical sense a smooth stress-strain curve for submicron sizes, but also that several corroborating indicators show the existence of a quite sharply defined threshold stress, presumably a material characteristic for a given specimen size and initial dislocation density.

More can be learned from the detailed analysis of the dislocation velocity distribution  $P(v)$ , done in 2D. We averaged over 5000 realizations the distribution of the absolute velocities of dislocations, at different load levels [see Fig. 4(a)]. Our main observation is that the tail of  $P(v)$  always decays as

$$P(v) \approx A v^{-\lambda}, \quad (1)$$

with exponent  $\lambda \approx 3 \pm 0.02$ .

The theoretical explanation of the cubic decay can be obtained under some natural assumptions about the correlation of dislocations. Previously it was shown that the

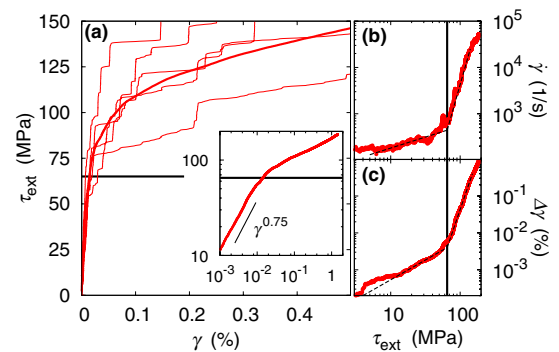


FIG. 2 (color online). Plastic responses in 3D. (a) Stress ( $\tau_{\text{ext}}$ ) versus plastic strain ( $\gamma$ ) curves of individual simulations (thin lines). The thick line is the average over realizations. The horizontal line marks the suggested critical yield stress. Inset shows the averaged curve on a log-log plot. (b) Mean deformation rate versus external stress. (c) Root mean square of strain fluctuations versus stress. Note that stress and time are equivalent.

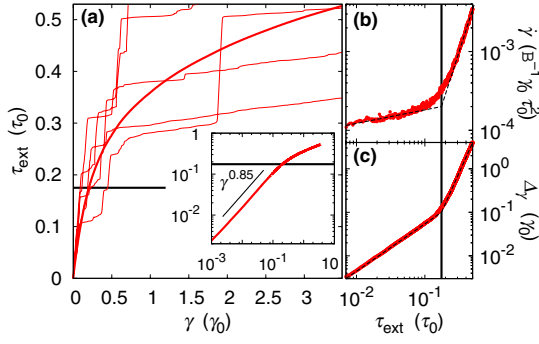


FIG. 3 (color online). Plastic responses in 2D. Panels (a)–(c) correspond to Figs. 2(a)–2(c), respectively. Quantities are in natural units defined in the text.

distribution of internal elastic stresses at a random location has a cubic tail [22]; presently, however, we are interested in the stress (proportional to the velocity) at the positions of dislocations. We give a simplified derivation first and then discuss its adaptation to our case. The cumulant generating function  $\Psi(q)$  of the stress distribution  $P(\tau)$  is given by

$$e^{\Psi(q)} = \int d\tau e^{iq\tau} P(\tau) = \langle e^{iq \sum_{n=1}^N \tau(r_n - r_0)} \rangle, \quad (2)$$

where the average is taken over the normalized joint distribution of  $N + 1$  dislocations  $f(\mathbf{r}_0, \dots, \mathbf{r}_N)$ , and  $\tau(\mathbf{r}) = r^{-1} \cos\varphi \cos 2\varphi$  is the stress field generated by a dislocation, in appropriate units, using polar coordinates. The large  $\tau$  behavior is determined by small  $q$ 's, so we keep the leading term in the Mayer cluster expansion

$$\Psi(q) \approx N \int (e^{iq\tau(r)} - 1) f(\mathbf{r}|\mathbf{0}) d^2r, \quad (3)$$

where the conditional distribution  $f(\mathbf{r}|\mathbf{0})$  appears. For  $r < q\epsilon$ , where  $\epsilon$  is small but fixed, the phase factor oscillates

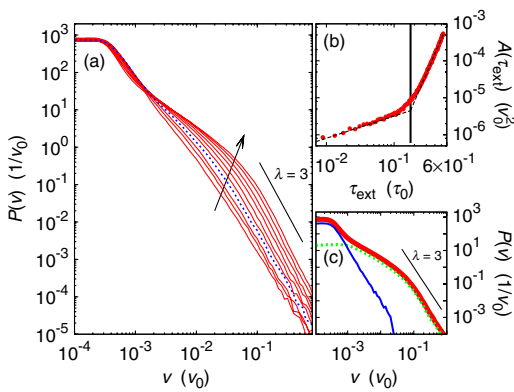


FIG. 4 (color online). (a) Dislocation velocity distributions at different external stress levels, increasing in the direction of the arrow. The dotted (blue) line corresponds to  $\tau_c$ . (b) The prefactor  $A(\tau_{\text{ext}})$  [see Eq. (1)] as a function of the external stress. (c) Above the yielding transition the velocity spectrum (thick red line) can be decomposed into the contribution of avalanches (dotted green line) and that of the quiescent configurations (thin blue line).

fast so the integral gives at most an order  $q^2$  contribution, if  $f$  is nonsingular. Setting the average of  $\tau$  to zero, the leading term comes from expanding in  $q$  as

$$\Psi(q) \approx -\frac{N}{2} q^2 \int_{r>q\epsilon} \tau^2(\mathbf{r}) f(\mathbf{r}|\mathbf{0}) d^2r \approx -\frac{\bar{A}}{2} q^2 \ln q, \quad (4)$$

where  $\bar{A} = N \int_0^{2\pi} \cos^2\varphi \cos^2 2\varphi f(r=0, \varphi|\mathbf{0}) d\varphi$ , provided the small-distance limit of  $f(r, \varphi|\mathbf{0})$  depends only on the angle. Note that  $1/f$  is of the order of area, so  $Nf$  is nonextensive. As the final step in the derivation one straightforwardly shows that the asymptote  $P(\tau) \approx \bar{A}\tau^{-3}$  yields by (2) the  $q$  dependence in (4). We mention that the cubic decay is a typical feature of x-ray line profiles [23].

Now we need to refine the above picture by the following considerations. First, there are two types of dislocations with  $\pm$  Burgers vectors, so pair correlations between all types have to be introduced, as it was worked out in [22]. Second, we should realize that the equilibrium correlation  $f_{\text{eq}}(\mathbf{r}|\mathbf{0})$  may diverge for small distances [24]. However, since dislocations do not move, the stress distribution is the Dirac delta centered at the origin, so  $\Psi_{\text{eq}}(q) \equiv 0$ . Thus we can use in (4) the time-dependent deviation from the equilibrium correlation. Note that the mathematical structure of the problem is similar to [22] and details will be published elsewhere. In conclusion, if the time-decaying term in the correlation produces a finite amplitude in (4) then the stress and thus the velocity distribution must have a reciprocal cubic decay.

Returning to the discussion of the simulations, the prefactor  $A$  in Eq. (1) was found to depend on the momentary external stress  $\tau_{\text{ext}}$ . According to Fig. 4(b),  $A(\tau_{\text{ext}})$  also undergoes a transition. Although the turn is not very sharp, the asymptotes apparently have different slopes, whose intersection point again gives  $\tau_c$  of Figs. 3(a)–3(c).

In a statistical sense, therefore,  $\tau_{\text{ext}} > \tau_c$  corresponds to the flowing regime, and  $\tau_c$  can be considered as a measure of the strength of the material for a given size. It should be stressed, however, that in an individual sample considerable dislocation motion may occur below  $\tau_c$ . For samples with macroscopic sizes,  $\tau_c$  is expected to go over to the conventional yield stress. Finally, we note that preliminary investigations suggest a weak rate dependence.

The investigations on the velocity distributions have also been repeated in 3D. Although in this case only a smaller ensemble can be afforded and the inherent numerical noise is much higher, there is a striking similarity between the 3D and the 2D results discussed above. The tail of the distribution is cubic, and its prefactor increases with the growing external stress. The emergence of the cubic decay indicates that its derivation in the 2D single-slip case actually has a much broader validity. Furthermore, as in 2D, the different distributions separate after a well-defined point and the small- $v$  part is nearly unaffected by the external stress.

The next issue to be considered is whether there is any mark of the avalanche activity on the velocity distribution

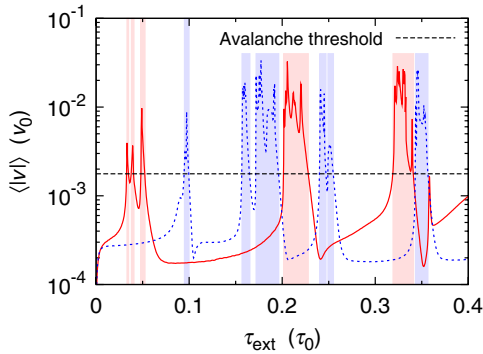


FIG. 5 (color online). Avalanches in the mean absolute velocity of dislocations versus stress (time). The two curves correspond to two different realizations. The horizontal line denotes the threshold value set for avalanche identification. The regions of avalanche state are marked by shading.

of dislocations. In an individual simulation, the system randomly alternates between quiescent and avalanche states, distinguished by a threshold (Fig. 5). As Fig. 4(c) shows it, the tail of the total velocity distribution comes from systems being in avalanche state, whereas quiescent states contribute only to the small- $v$  part of  $P(v)$ . The superposition of the two convex curves results in the characteristic “shoulder” in the distribution functions plotted in Fig. 4(a). Our investigations in 3D indicate that these similar features hold as well. In summary, the velocity distribution exhibits universality in more than one respect. First, the low-velocity part of the histogram is nearly independent of the external load. Second, the exponent of the decay at large velocities appears to be constantly 3 all along the loading scenario. Third, the critical yield stress manifests itself by an upturn in the amplitude of the power tail, due to increased avalanche weight.

While thus far we have analyzed peculiarities of the velocity distribution of dislocations, Orowan’s well-known law states that the plastic strain rate is proportional to the average dislocation velocity, weighted by the Burgers vector. So, it is natural to ask what the contribution is of the distribution tail obtained above, corresponding to avalanches, to the average plastic rate. We found that about 80% of the plastic strain rate is caused by dislocations with velocities beyond the onset of the shoulder. This implies that the fast dislocations forming avalanches play a dominant role in the plastic response. Furthermore, approximately 20% of the strain rate comes from the power-decaying part, significant for a tail.

We emphasize that small scale dislocation simulations abound from the past 30 years. On the other hand, experiments were available only on macroscopic plasticity, in sizes never reached by simulations. In this Letter the two approaches meet: now that experiments reached down to submicron level, simulations become more faithful.

Increased computer power made it possible to describe ensembles never considered before; thus, a statistical analysis with new conclusions and definition of the yield stress in small scale specimens could be reached.

The authors thank G. T. Zimányi for illuminating comments. G. G. is indebted to M. Droz for hospitality at the University of Geneva. Support of the OTKA Grant No. K 67778 and the Swiss NSF is acknowledged.

\*ispanovity@metal.elte.hu

- [1] M.-C. Miguel, A. Vespignani, S. Zapperi, J. Weiss, and J.-R. Grasso, *Nature (London)* **410**, 667 (2001).
- [2] J. Weiss and D. Marsan, *Science* **299**, 89 (2003).
- [3] M. D. Uchic, D. M. Dimiduk, J. N. Florando, and W. D. Nix, *Science* **305**, 986 (2004).
- [4] D. M. Dimiduk, C. Woodward, R. LeSar, and M. D. Uchic, *Science* **312**, 1188 (2006).
- [5] S. Brinckmann, J.-Y. Kim, and J. R. Greer, *Phys. Rev. Lett.* **100**, 155502 (2008).
- [6] M. Zaiser, J. Schwerdtfeger, A. S. Schneider, C. P. Frick, B. G. Clark, P. A. Gruber, and E. Arzt, *Philos. Mag.* **88**, 3861 (2008).
- [7] F. F. Csikor, C. Motz, D. Weygand, M. Zaiser, and S. Zapperi, *Science* **318**, 251 (2007).
- [8] B. Devincere, T. Hoc, and L. Kubin, *Science* **320**, 1745 (2008).
- [9] M. Koslowski, R. LeSar, and R. Thomson, *Phys. Rev. Lett.* **93**, 125502 (2004).
- [10] M. Zaiser and P. Moretti, *J. Stat. Mech.* (2005) P08004.
- [11] H. M. Jaeger, S. R. Nagel, and R. P. Behringer, *Rev. Mod. Phys.* **68**, 1259 (1996).
- [12] B. Gutenberg and C. F. Richter, *Bull. Seismol. Soc. Am.* **34**, 185 (1944).
- [13] S. Zapperi, A. Vespignani, and E. Stanley, *Nature (London)* **388**, 658 (1997).
- [14] G. Blatter, M. V. Feigel’aman, V. Geshkenbein, A. Larkin, and V. Vinokur, *Rev. Mod. Phys.* **66**, 1125 (1994).
- [15] P. Sammonds, *Nature Mater.* **4**, 425 (2005).
- [16] P. Bak, C. Tang, and K. Wiesenfeld, *Phys. Rev. A* **38**, 364 (1988).
- [17] J. P. Sethna, K. A. Dahmen, and C. R. Myers, *Nature (London)* **410**, 242 (2001).
- [18] M.-C. Miguel, A. Vespignani, M. Zaiser, and S. Zapperi, *Phys. Rev. Lett.* **89**, 165501 (2002).
- [19] D. Weygand, L. H. Friedman, E. van der Giessen, and A. Needleman, *Model. Simul. Mater. Sci. Eng.* **10**, 437 (2002).
- [20] See supplementary material at <http://link.aps.org/supplemental/10.1103/PhysRevLett.105.085503> for example simulation movies.
- [21] B. Bakó, I. Groma, G. Györgyi, and G. T. Zimányi, *Phys. Rev. Lett.* **98**, 075701 (2007).
- [22] I. Groma and B. Bakó, *Phys. Rev. B* **58**, 2969 (1998).
- [23] I. Groma, *Phys. Rev. B* **57**, 7535 (1998).
- [24] I. Groma, G. Györgyi, and B. Kocsis, *Phys. Rev. Lett.* **96**, 165503 (2006).